Bulk- and surface-plasmon-loss intensities in photoelectron, Auger, and electron-energy-loss spectra of Al metal

P. M. Th. M. van Attekum and J. M. Trooster
Department of Physical Chemistry, University of Nijmegen, Toernooiveld, Nijmegen, The Netherlands
(Received 7 April 1978)

The intensities of plasmon-loss satellites of core lines and the valence band in x-ray-photoemission spectra (XPS), as well as of Auger lines of Al are determined by convoluting the no-loss spectra with an asymmetric Lorentzian line shape. Intrinsic processes contribute 25% of the total plasmon intensity of XPS core lines. For the valence band the intrinsic process is noticeably less and contributes approximately 12%. For the *KLL* and *KLV* Auger lines the intrinsic processes have the same contribution as for the XPS core lines. The extrinsic plasmon-loss intensity is measured independently on electron-energy-loss spectra. The line shape of the plasmon losses in the latter is different from that in x-ray photoemission and Auger spectra, and both are different from theoretical plasmon energy distribution functions. The importance of intrinsic processes is confirmed by the observation of a plasmon gain line in the *KLL* Auger spectrum.

I. INTRODUCTION

The existence of collective electron density oscillations (plasmons) is known since the theoretical work of Pines and Bohm.[1-3] Since that time many experimentalists using different techniques have studied these plasmons, especially in the free-electron metals, where the plasmons manifest themselves most clearly. For Al metal many studies have been published using optical,[4] energy-loss,[5,6] and electron-transmission[7-9] techniques. In all these experiments the excitation of the plasmon occurs during the transport of the electron through the solid, the so-called extrinsic plasmon excitation. In x-ray photoemission a second kind of plasmon excitation is possible, the so-called intrinsic process, where the excitation of the plasmon takes place simultaneously with the creation of the hole. Both contributions can be separated by an analysis of the area intensity of the subsequent plasmon-loss lines.[10,11] Since the intrinsic process is believed to contribute only a minor part to the plasmon intensity a careful analysis is necessary. In the present study on Al metal the plasmons accompanying the $2s$ and $2p$ core levels, the valence band and the x-ray-excited *KLL* and *KLV* Auger lines will be discussed. Furthermore results of electron-energy-loss (EEL) experiments will be given. The plasmon losses of the core and valence-band photoelectron spectra have been studied earlier[10-14] and we will comment on this work in connection with our results in Sec. IV.

In Sec. II the experimental aspects of our investigation are given. In Sec. III the experimental results are analyzed. Finally the results are discussed in Sec. IV.

II. EXPERIMENTAL

X-ray-photoelectron, Auger, and EEL spectra were measured in a Leybold-Hereaus LHS-10 spectrometer. The excitation source for the x-ray photoelectron and Auger spectra was a Henke-type x-ray tube with Mg anode operated at 200 W. The $K\alpha_{1,2}$ line of Mg has too low energy for photoionization of the Al K shell, but the bremsstrahlung background proved to be of sufficient intensity to enable the study of the *KLL* and *KLV* Auger transitions. The x rays illuminate the sample under an angle of 60° with the normal to the surface. Electrons escaping from the sample along the normal to the surface are retarded and focused by an electron lens on the entrance slit of a hemispherical analyzer set for a constant pass energy.[15] The spectra were measured by repeated scans of 1 min and stored in a multichannel analyzer. The x-ray satellite lines in the photoelectron spectra were removed with a computer program described elsewhere.[16] The EEL spectra were measured with primary electrons impinging on the surface under an angle of 60° with the normal. The energy width of the primary electrons was less than 0.5 eV.

The samples were prepared in a preparation chamber by evaporation on a polished stainless-steel plate at a pressure of $\sim 10^{-6}$ Pa. Immediately after the evaporation the sample was slid into the measuring chamber through a valveless lock. The pressure during the measurements was less than 10^{-9} Pa. The samples were free of impurities, no carbon or oxygen could be detected.

III. RESULTS AND ANALYSIS

A. X-ray photoelectron spectra

X-ray-photoelectron spectrum of the $2s$ and $2p$ levels of Al metal with accompanying plasmon-loss lines is shown in Fig. 1(a). This spectrum was measured with a transmission energy of 50 eV, which results in an instrumental line shape which

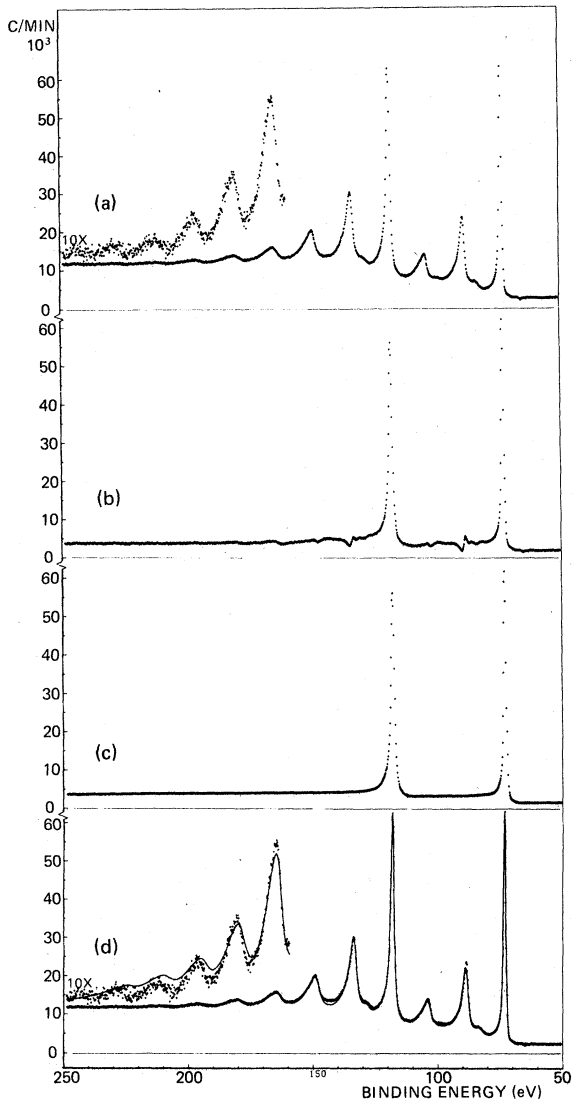

FIG. 1. Photoemission spectrum of the 2*s* and 2*p* core levels of Al metal. The spectrometer transmission energy was 50 eV; number of channels was 1024. (a) Experimental spectrum after correction for x-ray satellites. (b) After removal of the contributions of the plasmon-loss lines using the parameters of Table I. (c) The same as (b) after baseline smoothing. (d) Comparison between experimental (points) and calculated plasmon-loss spectrum (solid line) using the parameters of Table I and (c) as zero-loss spectrum.

is Lorentzian with a linewidth of 0.60 eV.[17] Apart from the bulk-plasmon-loss lines, a surface-plasmon-loss line can be clearly discerned. In judging the intensity of the surface-plasmon-loss line it should be kept in mind, that electrons are measured, that escape at right angles to the surface. The binding energies are: 118.1 ± 0.1 eV for the 2*s* and 73.0 ± 0.1 eV for the 2*p* line. These values are the mean of three independent measurements and in good agreement with those published earlier.[18-20] The asymmetric line shape of the no-loss lines is a consequence of electron-hole excitations and has been extensively discussed by Citrin *et al.*[21] The plasmon-loss peaks are also markedly asymmetric. The shape of the plasmon-loss lines has been discussed by Hedin[22] and Penn.[12-14] However, we found that the theoretical line shape of Hedin or Penn could only reproduce the main features of the measured spectra (see below). Therefore and for computational reasons a simpler analytical expression was used to describe the asymmetrical plasmon-loss lines, using the following assumptions:

(a) The nth bulk-plasmon-loss line P_n is given by the convolution of the no-loss line P_0 with the plasmon-loss energy distribution function $D_n(E)$:

$$P_n(E) = P_0(E) * D_n(E) . \tag{1}$$

(b) $D_n(E)$ is given by an asymmetric Lorentzian

$$D_n(E) = \frac{I_n}{1 + [(E - E_n)/\Gamma_n(E)]^2} . \tag{2}$$

Asymmetry is obtained by taking $\Gamma_n(E) = \Gamma_n^R$ for $E < E_n$ and $\Gamma_n(E) = \Gamma_n^L$ for $E > E_n$.

(c) To reduce the number of parameters the following relations were assumed to hold:

$$\Gamma_n^{R,L} = n\Gamma^{R,L} , \tag{3a}$$

$$E_n = nE_B . \tag{3b}$$

E_B is the bulk-plasmon energy.

(d) The surface-plasmon energy distribution function is similarly described by

$$P_S(E) = P_0(E) * D_S(E) , \tag{4}$$

with $D_S(E)$ also given by an asymmetric Lorentzian with parameters I_S, Γ_S^L, Γ_S^R, and E_S.

(e) Lines due to a combination of bulk- and surface-plasmon losses are given by

$$P_{S,n}(E) = P_0(E) * D_{S,n}(E) , \tag{5}$$

where $D_{S,n}$ is an asymmetric Lorentzian for which

$$\Gamma_{S,n}^{R,L} = \Gamma_n^{R,L} + \Gamma_S^{R,L} , \tag{6a}$$

$$E_{S,n} = nE_B + E_S , \tag{6b}$$

$$I_{S,n} = I_n I_S . \tag{6c}$$

(f) Multiple surface-plasmon losses are neglected.

In Ref. 16 a method was given to determine the positions and intensities of the x-ray satellite lines in an x-ray-photoelectron spectrum. With the assumptions given above the same method can be used to determine the parameters I_n, Γ^R, Γ^L, E_B, I_S, Γ_S^R, Γ_S^L, E_S. Starting from the right in

Fig. 1(a) we can remove from the spectrum the intensity due to plasmon excitations using the algorithm described in Ref. 16. The best values of the parameters were determined with a least-squares fitting procedure[23] with the requirement that the spectrum to the left of the $2s$ line should approach the tail of a Lorentzian of linewidth 1.75 eV and intensity 55 000 counts/min, superimposed on an adjustable constant term. Although the least-squares fitting was restricted to the part of the spectrum left of the $2s$ line the contribution in this region of the plasmon-loss lines associated with the $2p$ line were taken into account. Seven plasmon-loss lines of each x-ray-photoelectron spectrum line have been included in the fitting procedure. Fits have been made to three independent measurements. Figure 1(b) gives the spectrum obtained after removal of the plasmon-loss lines using the parameters given in Table I. Smoothing the spectrum of Figure 1(b) one obtains the spectrum of Figure 1(c) which was used to generate the calculated plasmon-loss spectrum shown in Figure 1(d) together with the measured data. A good fit is obtained up to the fourth plasmon-loss line. The value of E_B is in good agreement with the results of Williams *et al.*[24] who found $E_B = 15.2$ eV, but somewhat smaller than found by Pollak *et al.*[19] [$E_B = 15.7(2)$ eV] and Flodstrom *et al.*[20] ($E_B = 15.7$ eV). The ratio $E_B/E_S = 1.47$ is close to the theoretical value 1.41.

TABLE I. Best parameter values for the plasmon losses in Al metal. The peak intensity (I_n, I_s) is given in percentage units of the no-loss peak per ΔE, where ΔE is the energy increment per channel. Errors are given in units of the last decimal.

Parameter	Value	Units
I_1	24.6(5)	$\%\,\mathrm{eV}^{-1}$
I_2	8.4(3)	$\%\,\mathrm{eV}^{-1}$
I_3	3.6(2)	$\%\,\mathrm{eV}^{-1}$
I_4	1.6(1)	$\%\,\mathrm{eV}^{-1}$
I_5	0.8(1)	$\%\,\mathrm{eV}^{-1}$
I_6	0.4(1)	$\%\,\mathrm{eV}^{-1}$
I_7	0.2(1)	$\%\,\mathrm{eV}^{-1}$
I_S	5.0(2)	$\%\,\mathrm{eV}^{-1}$
Γ^L	1.52(5)	eV
Γ^R	0.60(5)	eV
Γ_S^L	1.4(1)	eV
Γ_S^R	0.5(1)	eV
E_B	15.32(5)	eV
E_S	10.41(5)	eV

The following points should be noted:

(a) The plasmon-loss lines are calculated as a convolution with the no-loss line. The parameters of $D_n(E)$ are therefore a direct measure of the shape, area intensity, and position of the plasmon-loss lines relative to the zero-loss line and are independent of the shape of the latter.

(b) The "misfit" as apparent in Fig. 1(b) is of a derivative character. Hence the area intensities of the calculated lines are a better measure of the intensity than is suggested by the absolute deviations present in Fig. 1(b).

(c) The inclusion in the fit of a constant term which raises the baseline on the left of the $2s$ line introduces an uncertainty in the intensities of the plasmon-loss lines. This baseline presumably is due to inelastic scattering of the photoelectrons other than plasmon excitation. The reliability of the results however is supported by the good fit obtained for the first two plasmon-loss lines of the $2p$ line, which were not included in the sum of least squares. Note that the $2p$ line is considerably narrower than the $2s$ line.

(d) To a very good approximation the $2s$ and $2p$ lines in Fig. 1(c) can be described with a Doniach-Sunjic line shape over the same range as used by Citrin *et al.*[21]

(e) The intensity between the first and second bulk-plasmon-loss line could not be fitted appropriately with the constraints described above. It appears that the intensity of the first bulk-surface plasmon loss is higher as given by Eqs. (5) and (6).

Following Pardee *et al.*[10] the area intensity of the nth plasmon-loss line is given by

$$A_n = \alpha^n \sum_{m=0}^{n} \frac{(\beta/\alpha)^m}{m!} \quad , \tag{7}$$

TABLE II. Experimental area intensities of the bulk and surface-plasmon losses compared with theoretical values from Eq. (7) with $\alpha = 0.62$ and $\beta = 0.21$. The area intensity is listed in percentage units of the no-loss line and given by $A_n = \frac{1}{2}\pi\,(\Gamma_n^L + \Gamma_n^R)\,I_n$.

Parameter	Experiment %	Theory %
A_1	82 ± 2	83
A_2	56 ± 2	54
A_3	36 ± 2	34
A_4	21 ± 2	21
A_5	13 ± 3	13
A_6	8 ± 3	8
A_7	5 ± 3	5
A_S	15 ± 3	•••

where $\alpha = (1 + l/L)^{-1}$, l is the mean free path for extrinsic plasmon excitation, L is the mean attenuation length for electrons due to processes other than plasmon excitation. The parameter β is a measure for the probability $P_i(n)$ for intrinsic excitation of n plasmons:

$$P_i(n) = e^{-\beta}(\beta^n/n!) . \quad (8)$$

By least-squares fitting Eq. (7) to the experimental area intensities A_n as derived from the parameters listed in Table I, we found $\alpha = 0.62$ and $\beta = 0.21$. In Table II both measured and calculated values of A_n are given. With these values the total intensity in the bulk-plasmon-loss lines is 2.3 times the intensity in the no-loss line and the intrinsic process contributes 25% of the total plasmon intensity. An estimate of the effect of the baseline on α and β was made by correcting the peak intensities of the plasmon-loss lines with the value of the baseline constant: either α or β changed by about 10%.

The surface-plasmon-loss intensity A_s is very close to the theoretical estimate.[25] This is an indication of the high purity of the surface: even very slight oxidation reduces the surface-plasmon intensity appreciably. The ratio $A_s/A_1 = 0.18$ is larger than the value which was found by Williams *et al.*[24] through extrapolation of angle dependent measurements. It should be remarked, that the area intensity of the third plasmon-loss line of the $2p$ line is approximately 25% of the $2s$ line, with which it nearly coincides. Therefore neglect of this line in analyzing the line shape of the $2s$ line, as is done by Citrin *et al.*,[21] is not allowed.

B. X-ray photoelectron valence band spectra

As mentioned before, the determination of the plasmon parameters is independent of the line shape of the no-loss line. The same algorithm as was used to obtain the difference spectrum of Fig. 1(b) can therefore be used to remove the plasmon-loss peaks of the valence-band spectrum.

Figure 2(a) shows again the spectrum of the $2s$

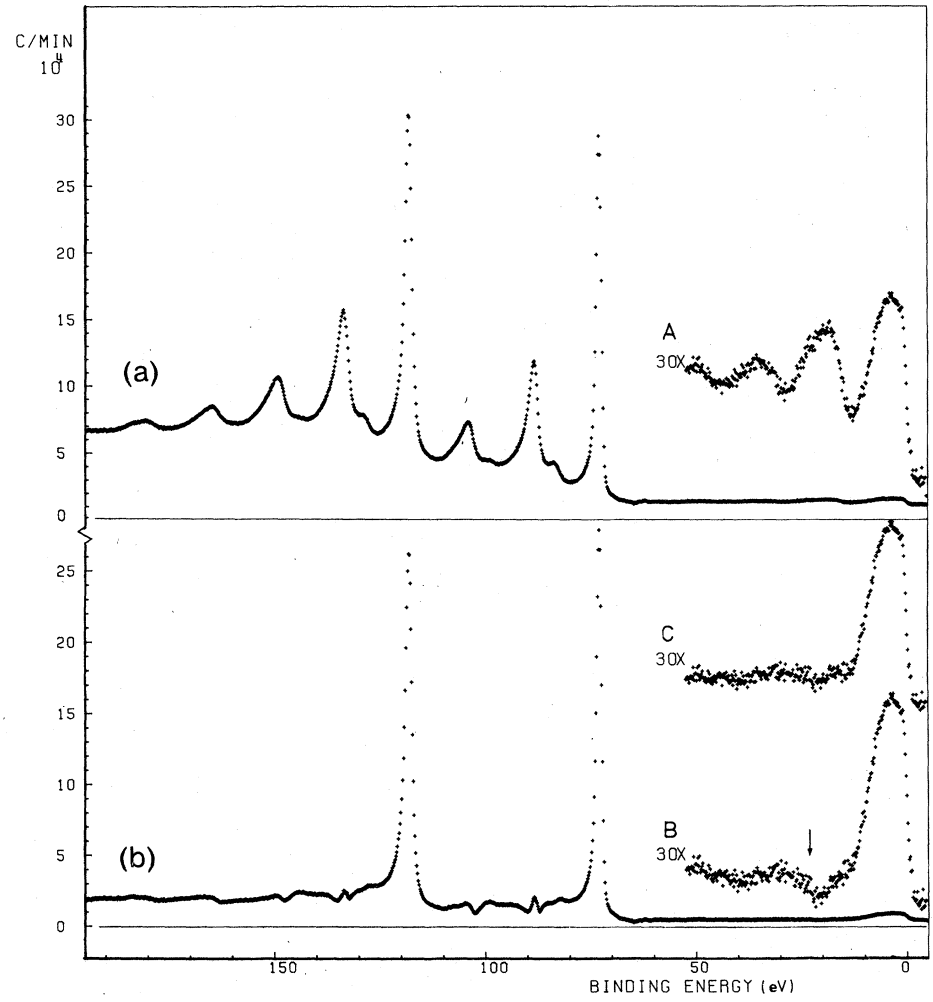

FIG. 2. Photoemission spectrum of the $2s$ and $2p$ core levels and valence band of Al metal. The spectrometer transmission energy was 150 eV. (a) Experimental spectrum after correction for x-ray satellites. (b) After removal of the contribution of the plasmon-loss lines using the parameters of Table I (e.g., $\beta = 0.21$). (c) After removal of the plasmon-loss lines with $\beta = 0.10$, for the valence-band region.

and $2p$ lines but this time including the valence band. This spectrum was measured with a lower resolution than that of Fig. 1(a), which results in a higher count rate. Figure 2(b) is obtained by removing the plasmon-loss lines using the parameters given in Table I. The spectrum to the left of the $2s$ and $2p$ lines closely resembles that of Fig. 1(b). This demonstrates the line-shape independence of the method. However, for the valence band the subtracted plasmon intensity is too high. At the site of both the first and second plasmon-loss line the intensity in Fig. 2(b) is too low. This effect was observed in two independent measurements. Oxidation of the sample can be excluded as the cause: The bulk plasmon intensity is not very sensitive to oxidation and even a slightly oxidized sample should give an O($2s$) line at the site of the arrow in Fig. 2(b). Therefore we believe that this is evidence of the fact that for valence-band electrons the intrinsic plasmon intensity is less than for core electrons: Using intensities calculated with $\beta = 0.1$ the spectrum given in Fig. 2(c) is obtained. This method of removing plasmon-loss intensity gives also better insight in the true shape of the valence-band x-ray-photoelectron spectrum. In Fig. 3 we compare the shape of the valence band as determined by us with that of Baer and Busch[26] which has been used in many discussions. Especially at the high binding energy side there is considerable

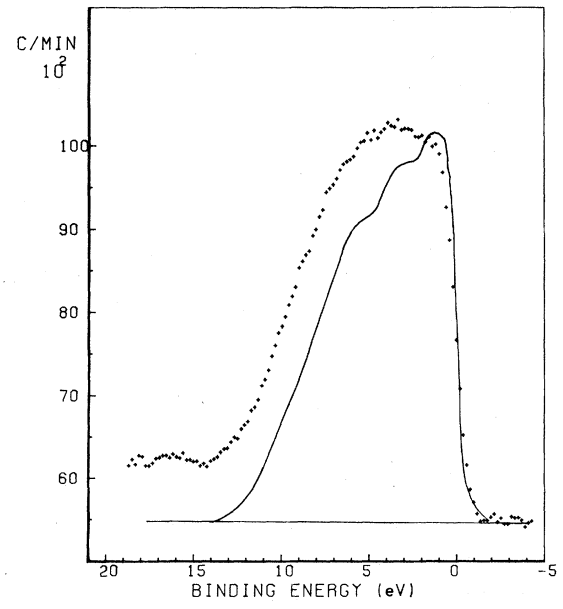

FIG. 3. Valence band of Al metal after removal of plasmon-loss lines. The solid line is taken from the work of Baer and Busch (Ref. 26). Spectrometer transmission energy was 150 eV.

difference, which is due to the fact, that Baer and Busch have made no correction for surface- or bulk-plasmon-loss lines but simply subtracted a slanted baseline from the measured spectrum.

C. Auger spectrum

In Fig. 4 we give the Auger lines in the region from 1300 to 1500 eV. This covers all but one of the KLL and all KLV transitions. Table III lists our values for the kinetic energies (corrected for the work function) together with theoretical and experimental data by Dufour *et al.*[27] For the KLL transitions there is good agreement. No literature data are available for the KLV transitions.

In Fig. 4(b) we have subtracted the plasmon-loss lines, again using the parameters of Table I. For the KLL transitions the deviations from a smooth line are of similar shape and magnitude as in Fig. 1(b). We conclude therefore, that the intensities of the plasmon-loss peaks are the same for x-ray-photoelectron spectra core lines and KLL Auger lines. The same appears to be true for the KLV lines: there is much less need for adjustment of the parameter β in this case. However, it should be pointed out, that the noise prevents an accurate determination of the plasmon-loss intensities for these lines.

Figure 4(b) reveals in a beautiful way the structure of the KLV Auger lines. A striking difference with the x-ray-photoelectron spectra valence band can be observed. The differences are similar to those observed in Mg,[28,29] and due to the fact that in the KLV Auger process emission occurs from the valence band as modified by the presence of the K hole. In extreme cases this can result in atomiclike Auger spectra.[30]

The Auger spectrum contains two more features which merit attention:

(a) The small peak marked A in Fig. 4(b) has an energy of 1413.7 eV and is due to internal photoemission from the Al $2p$ level: in the sample Al $K\alpha$ x rays of 1486.6 eV are generated through fluorescence decay of the holes in the K shell. These x rays in turn can lead to photoemission out of the $2s$ and $2p$ level. With a binding energy of 73 eV of the $2p$ electrons this results in a peak at ~1413.7 eV. The corresponding $2s$ line is difficult to discern because of the plasmon losses or what is left of those after their removal.

(b) The peak B has an energy of 1408.6 ± 0.5 eV and is broader than peak A. The energy difference with the $KL_{2,3}L_{2,3}$ (^1D) Auger transition is 15.4 ± 0.5 eV. This suggests that B is due to a plasmon gain peak. This interpretation is supported by the observation of a similar line in the Auger

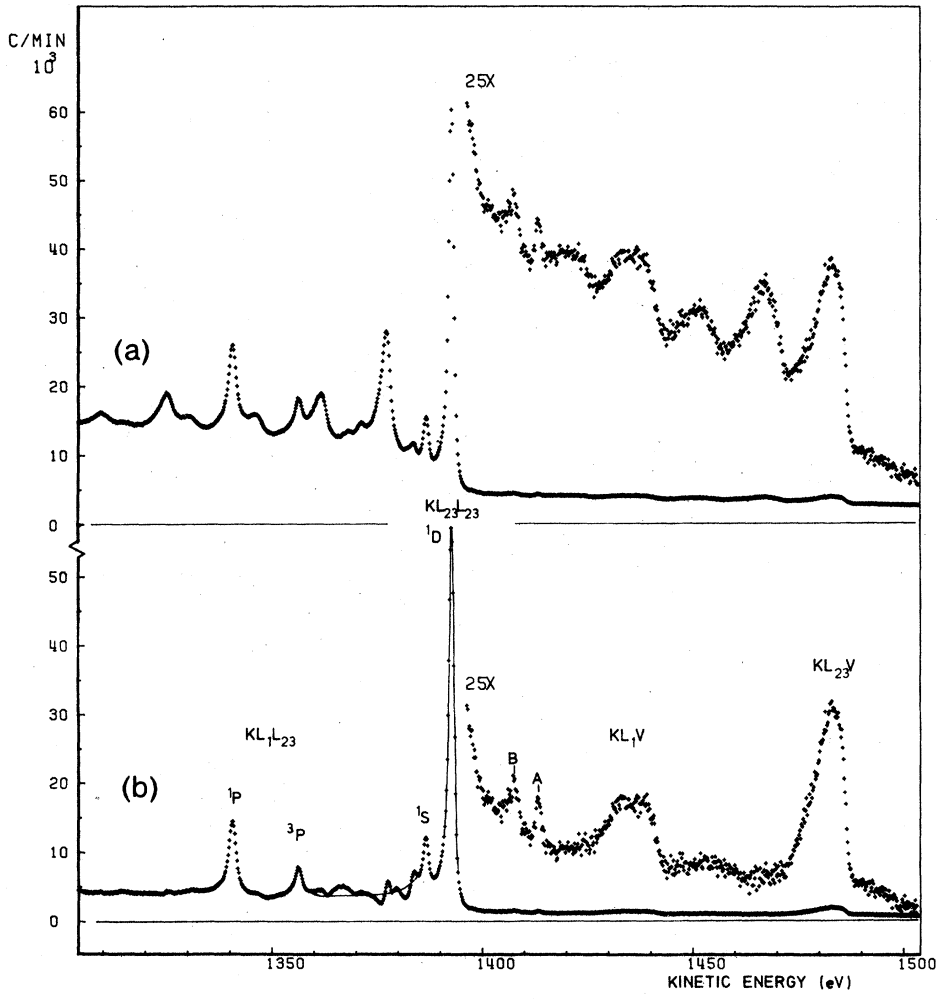

FIG. 4. X-ray excited KLL and KLV Auger spectrum of Al metal. The kinetic energy scale is corrected for the work function. (a) As measured; (b) after removal of the plasmon-loss lines using the parameters of Table I. A is the internal-photoemission Al $2p$ line, B a plasmon-gain peak of the $KL_{2,3}L_{2,3}$ (^1D) Auger line.

TABLE III. Kinetic energies (in eV), corrected for the work function, of the KLL and KLV Auger levels in Al metal. The values given in the second column are the mean of at least three measurements. Errors are given in units of the last decimal.

Peak	This work	Dufour *et al.* Experiment (Ref. 27)	Dufour *et al.* Theory (Ref. 27)
KL_1L_1 (^1S)	1302.0(2)	1302.0	1304.0
$KL_1L_{2,3}$ (^1P)	1341.2(2)	1341.4	1342.3
$KL_1L_{2,3}$ (^3P)	1356.8(2)	1357.2	1358.5
$KL_{2,3}L_{2,3}$ (^1S)	1387.1(2)	1387.2	1386.6
$KL_{2,3}L_{2,3}$ (^1D)	1393.2(2)	1393.2	1393.5
$KL_{2,3}L_{2,3}$ (^3P)	•••	•••	1398.1
KL_1M_1 $KL_1M_{2,3}$	1436.0(5)	•••	•••
$KL_{2,3}M_1$ $KL_{2,3}M_{2,3}$	1483.2(2)	•••	•••

spectra of Mg with an energy distance of 10.6 eV which is the plasmon energy for Mg.[31] The intensity of peak B is ~0.5% of the $KL_{2,3}L_{2,3}$ (^1D) Auger line. Plasmon gain peaks have been reported for the LVV Auger peaks,[32-34] but were later attributed to double ionization.[35,36] Double ionization can be excluded in our case because of the energy of the satellite and because low-intensity x rays were used as exciting radiation. According to Watts[37] and Almbladh[38] plasmon gain satellites are possible for Auger lines and connected with the intrinsic plasmon-losses occuring on the creation of the primary hole. According to Almbladh[38] the shorter lifetime of the K hole makes the occurrence of plasmon gain satellites more probable in KLL Auger spectra than in the LVV spectra studied up to now. Although the noise prevents an accurate determination of the line shape of the plasmon gain peak, the linewidth seems comparable to that of the plasmon-loss lines.

D. Electron-energy-loss spectra

EEL spectra were measured to obtain an independent determination of the parameter α in Eq. (7). In the EEL spectra intrinsic processes play no role and hence the area intensity ratio of successive plasmon-loss lines should be equal to α. Spectra were measured for primary energies ranging from 500 to 1500 eV. The intensity analysis of the EEL spectra is complicated by a background intensity due to inelastic scattering other than plasmon losses. This background increases in intensity with decreasing primary energy.

There is a striking difference in the shape of the plasmon-loss lines of the EEL and x-ray-photoelectron spectra: The lines appear to be more symmetrical and for primary energies greater than 750 eV narrower in the EEL spectra. This is partly due to the difference in shape of the no-loss line, but spectra calculated by con-

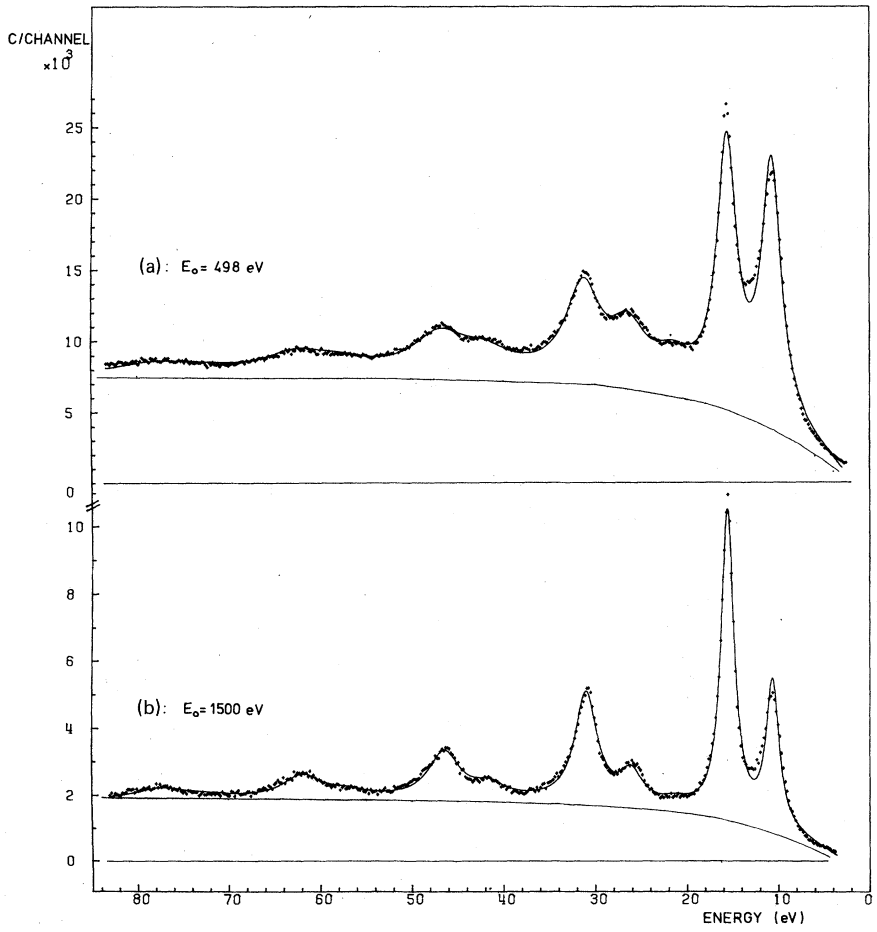

FIG. 5. EEL spectra of Al metal. (a) Fit of experimental spectrum (points) with symmetric Lorentzians at a primary energy of 498 eV. The baseline is indicated with a solid line. The zero of the energy scale corresponds with the position of the maximum of the no-loss line. (b) Same as (a) at a primary energy of 1500 eV.

voluting the measured no-loss peak of the EEL spectrum with the lineshapes of the plasmon-loss lines derived from the x-ray photoelectron spectrum result in broader plasmon-loss lines than observed. We have therefore fitted the measured EEL spectra with symmetrical Lorentzians. The background was approximated by $B(E) = b(1 - ae^{-(E-E_0)/c})$, E_0 is primary energy, b, a, and c are parameters to be fitted. Within each pair of bulk- and surface-plasmon-loss lines, P_n and $P_{S,n-1}$, the linewidth was kept equal: $\Gamma_n = \Gamma_{S,n-1}$ (see Sec. III A for definition symbols). Also the ratio $R = I_n/I_{S,n-1}$ was taken the same for all n, except for $n = 1$ because of the large uncertainty in the background under the first pair. The area intensity A_n of the nth bulk-plasmon-loss line was assumed to be given by $A_n = \alpha A_{n-1}$ for $n > 1$. Furthermore, a small peak corresponding with excitation of two surface plasmons was included in the fit. The peak intensity of this line (I_S^2) was used as a parameter, while the linewidth was fixed at $2\Gamma_1$. Thus the following adjustible parameters were used in the fit: I_1, I_S/I_1, R, I_S^2/I_1, α, Γ_n ($n = 1$ to 5), E_S, E_B, and the base-line parameters a, b, and c.

Figures 5(b) and 5(c) give the best fit for primary energies of 498 and 1500 eV and Table IV lists the parameter values obtained.

The following points should be noted: (a) The value of α is constant for primary energies ranging from 500 to 1500 eV and has the value 0.62 ± 0.02. This value of α is in excellent agreement with the value of α determined from the x-ray-photoelectron spectra. (b) The linewidth of the nth plasmon-loss line is given by $\Gamma_n = n\Gamma + \Gamma_0$, where $\Gamma_0 \simeq 0.5$ eV is the linewidth of the zero-loss line. Γ changes from 2.1 eV at 498 eV to 1.2 eV at 1500 eV. (c) The linewidth of corresponding plasmon-loss lines increases with decreasing primary energy. (d) The shape of the baseline is the same over the whole range (a and c are constant), but the intensity of the baseline relative to the intensity of the first plasmon-loss line (b/I_1) increases with decreasing primary energy. (e) The surface-plasmon-loss intensity is much higher than in the x-ray-photoelectron spectrum: This is due to the short penetration depth of the primary electrons and to the fact that the detected electrons have crossed the surface twice.

IV. DISCUSSION

This is not the first attempt to determine the intensities of plasmon-loss peaks in x-ray-photoelectron spectra and before discussing our results we comment briefly on some of the recent papers on this subject. The first attempt to determine the plasmon-loss intensities was made by Pardee *et al.*[10] These authors neglected the asymmetry of the plasmon-loss lines and fitted with Gaussians. Moreover the fact that the plasmon-loss lines are a convolution of the no-loss line with

TABLE IV. Best parameter values for the plasmon losses in the EEL spectra of Al metal as function of the primary energy E_0. Meaning of the symbols is given in the text. Errors are estimates based on several fits and given in units of the last decimal.

	$E_0 = 498$ eV	$E_0 = 751$ eV	$E_0 = 1000$ eV	$E_0 = 1252$ eV	$E_0 = 1500$ eV
E_B (eV)	15.7(1)	15.6(1)	15.6(1)	15.5(1)	15.5(1)
E_S (eV)	10.8(1)	10.6(1)	10.6(1)	10.6(1)	10.6(1)
I_S/I_1	0.99(5)	0.75(5)	0.60(5)	0.55(5)	0.47(5)
R	0.53(5)	0.40(5)	0.36(5)	0.30(5)	0.28(5)
I_S^2/I_1	0.19(3)	0.11(3)	0.08(3)	0.06(3)	0.04(3)
α	0.62(2)	0.61(2)	0.63(2)	0.63(2)	0.61(2)
Γ_1(eV)	2.6(1)	2.1(1)	2.0(1)	1.9(1)	1.7(1)
Γ_2(eV)	4.5(1)	3.6(1)	3.4(1)	3.2(1)	2.9(1)
Γ_3(eV)	6.9(2)	5.5(2)	5.1(2)	4.5(2)	4.2(2)
Γ_4(eV)	8.4(3)	7.7(3)	6.7(3)	6.0(3)	5.2(3)
Γ_5(eV)	10.4(4)	11.2(4)	8.0(4)	8.0(4)	7.0(4)
a	1.27(3)	1.21(3)	1.30(3)	1.40(3)	1.35(3)
c (eV)	11.0(3)	10.1(3)	9.6(3)	10.2(3)	11.4(3)
I_1/b	9.4(1)	10.6(1)	13.0(1)	13.1(1)	13.2(1)

the plasmon energy distribution function was not taken into account. The same approach was used by Williams *et al.*[24] in a study of the angular dependence of the plasmon intensities. A rough analysis was made by Fuggle *et al.*[39] More recently Steiner *et al.*[11] have published results on Be, Na, Mg, and Al. For Al these authors find $\alpha = 0.67$ and $\beta = 0.10$. However, no details of the fitting procedure are given. According to the same authors the same parameters as used for the core lines give good results for the valence-band spectra of Be, Na, and Mg.[40] However, these good fits are obtained including a background correction, which assumes a background proportional to the integrated intensity. As pointed out recently by Citrin *et al.*[21] there is no experimental basis for this correction.

In all these cases Al $K\alpha$ radiation was used. However, the plasmon-loss intensities are not expected to depend much on the kinetic energy of the photoelectrons. A comparison between spectra obtained by us with Mg $K\alpha$ and Al $K\alpha$ radiation did not reveal marked differences.

In a series of papers Penn has used a fundamental approach, calculating intensities and line-shapes from theory.[12-14] The bulk plasmon line shape, $P(E,E')$, was derived from the Lindhard dielectric function $\epsilon(q,\omega)$:

$$P(E,E') = \frac{v(E)}{\pi a_0 E} \int \frac{dq}{q} \operatorname{Im}\left(\frac{1}{\epsilon(q,E-E')}\right). \quad (9)$$

with

$$\operatorname{Im}[1/\epsilon(q,\omega)] = \omega_p^2 \omega \tau_q / [(\omega^2 - \omega_q^2)^2 + (\omega\tau_q)^2]. \quad (10)$$

ω_p is the plasmon frequency for wave vector $q = 0$, τ_q is a measure for the lifetime broadening, which is related to the linewidth of the plasmons. Gibbons *et al.*[41] determined experimentally the linewidth of the plasmons in Al as function of the wave vector

$$\Gamma(\omega_q) = 0.9 + 3.25 q^2, \quad (11)$$

where $\Gamma(\omega_q)$ is expressed in eV and q in Å^{-1}. The relation between the plasmon energy $\hbar\omega_q$ and q is given by[9,41]

$$\hbar\omega_q = \hbar\omega_p + 3.01 q^2. \quad (12)$$

We have calculated numerically the line shape resulting from Eq. (9). The result is shown in Fig. 6. In two consecutive papers Penn was able to obtain good fits to experimental data with[13] and without[12] inclusion of intrinsic processes. In a recent paper the plasmon losses of the valence band were analyzed.[14] However, using the line shape of Fig. 6 we were not able to reproduce the measured spectrum very well. This is illustrated in Fig. 7(a). To obtain the calculated spectrum

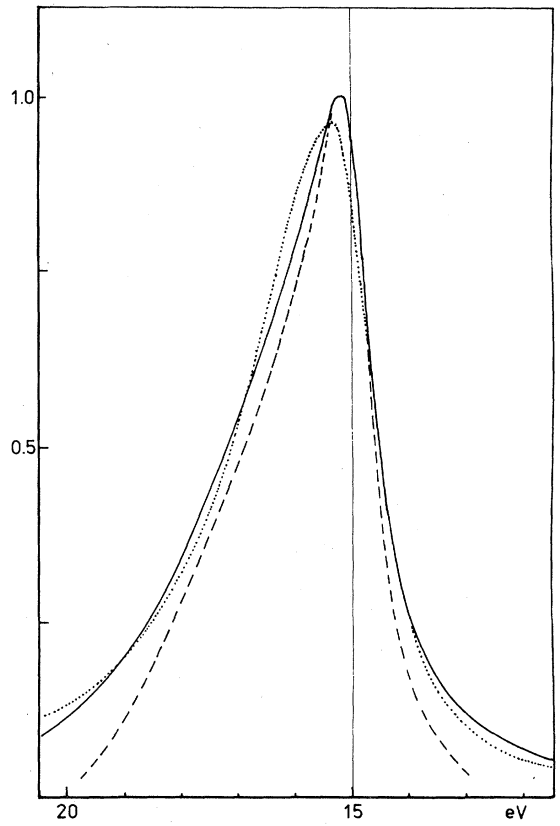

FIG. 6. Plasmon energy distribution function calculated with the model of Penn [Eq. (9)] (dashed line), the model of Hedin [Eq. (13)] (solid line). In both cases $\hbar\omega_p = 15.0$ eV. Also given is the asymmetric Lorentzian (dotted line) fitted to the curve of Hedin. This line has $\Gamma^L = 1.88$ eV and $\Gamma^R = 0.76$ eV.

self-convolutions of the line shape from Eq. (9) were calculated numerically and convoluted with the spectrum of Fig. 1(c). Obviously the main cause for the discrepancy is a too low intensity in the wings of the line shape of Eq. (9), but two other points are noteworthy: the line shape of the second and higher plasmon-loss peaks is more symmetric than measured and the maxima of the plasmon-loss peaks are shifted to the left.

Hedin[22] has given a different expression for the plasmon energy distribution function:

$$g(\omega) = (e^2/\pi)\,(\tfrac{1}{2}m)^{1/2}\,[\omega_p^2\,\Theta(\omega-\omega_p)/\omega^3(\omega-\omega_p)^{1/2}] \quad (13)$$

To include lifetime effects this function was convoluted with a Lorentzian with linewidth depending on ω_q as given by Eqs. (11) and (12). The result of a numerical calculation of Hedin's function is also given in Fig. 6. The main difference with Penn's function is the larger intensity in the wings, which is the result of the more realistic Lorent-

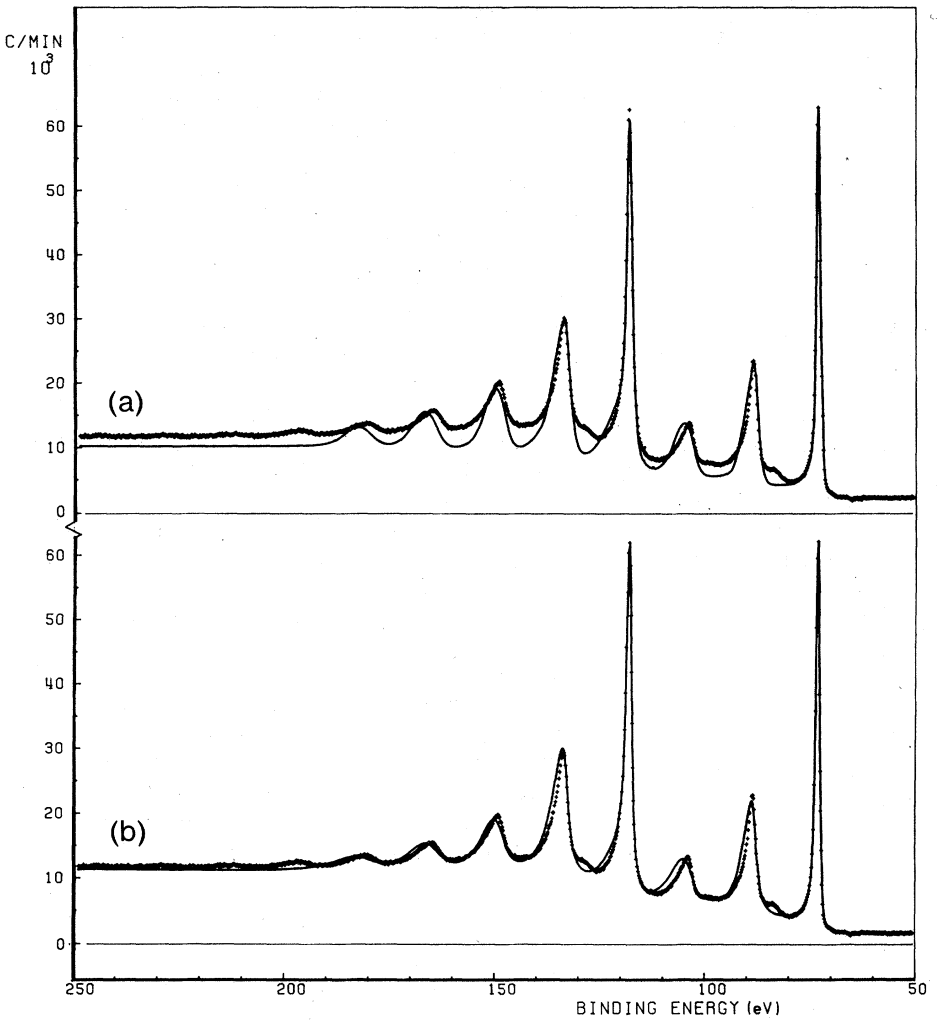

FIG. 7. Comparison between experimental spectrum and theoretical models of Penn (a) and Hedin (b). The drawn lines are convolutions of Fig. 1(c) with the theoretical line shapes given in Fig. 6 and self-convolutions thereof. The peak intensity ratio I_n/I_1 was taken equal to the value resulting from Table I and I_1 was scaled to give reasonable fit to the first plasmon-loss line. Only bulk-plasmon-loss contributions were taken into account.

zian lifetime broadening as compared to Eq. (9). Also shown in Fig. 6 is an asymmetric Lorentzian line shape as used in our analysis, which gives the best fit to Hedin's function. It is clear that the asymmetric Lorentzian is a good approximation of Hedin's function. In the same way as described above the plasmon-loss spectrum was calculated with Hedin's function. Figure 7(b) shows the result; there is better agreement with the measured spectrum than with Penn's approach. However, again the line shape of the second and higher plasmon-loss peak is too symmetric and the maxima are shifted to the left as compared with the experimental data. As can be seen in Fig. 1(d) such a shift is indeed observed but becomes appreciable only in the fifth and higher plasmon-loss lines (Remember that the fitted spectrum of Fig. 1(d) was constrained to have equidistant plasmon-loss lines).

It is important to note that the plasmon energy distributions $D_n(E)$, which we have used to fit the second and higher plasmon-loss lines, are not self-convolutions of the energy distribution of the first plasmon-loss line $D_1(E)$, as expected from theory when spatial redistribution on scattering is neglected. This is assumed to be valid for the x-ray-photoelectron and Auger spectra because the initial direction of the unscattered electron is undetermined and for the EEL spectra because they are obtained on polycrystalline materials. Similarly unexplained is the observation that the plasmon-loss line shape is different for EEL and x-ray-photoelectron spectra.

The x-ray-photoelectron spectra and EEL measurements give two independent determinations of α, which are in excellent agreement with each other. The fact that α is constant for the energy range 500–1500 eV is in agreement with results

by Flodstrom *et al.*[20] who measured the bulk plasmon intensities for kinetic energies between 30 and 330 eV. The plasmon intensity appears to be constant above 200 eV. The same authors give a theoretical estimate of $\alpha = (1 + l/L)^{-1}$ which for energies larger than 200 eV results in $\alpha = 0.64$ again in excellent agreement with our results.

The value of β obtained is in effect an effective number. As shown by Langreth[42] and Gadzuk[43] the intrinsic plasmon satellites are weakened by the presence of interference effects between intrinsic and extrinsic plasmon excitations. However, as shown by these authors, Eq. (7) can still be used. The relatively large intrinsic contribution for core electrons found in our analysis is supported by the observation of a plasmon gain satellite of the $KL_{2,3}L_{2,3}$ (^1D) transition. The smaller intrinsic plasmon excitation in the case of the valence band is not unexpected for delocalized electrons. Penn[14] had discussed mechanisms which can lead to intrinsic plasmon-losses of the valence electrons, but in the light of our results his calculation overestimates the importance of these effects. It is surprising that for Auger lines and x-ray-photoelectron spectra core lines essentially the same intensities are found for the plasmon-loss lines. The fact that there seems to be no need for reduction of the intrinsic contribution in case of the KLV Auger lines may be understood by the polarization of the valence electrons by the K hole.

V. CONCLUSIONS

The results of this investigation can be summarized as follows: (i) Using asymmetric Lorentzians to describe the line shape of the plasmon-losses good fits to the experimental x-ray-photoelectron core level spectra could be obtained. From the area intensities of the plasmon-loss lines we derive for the extrinsic (α) and intrinsic (β) contribution to the plasmon excitations $\alpha = 0.62$ and $\beta = 0.21$. This means, that the intrinsic plasmon excitation contributes at least 25% to the total of the plasmon excitations. (ii) The theoretical line shape of Penn can only reproduce the main features of the measured spectra, Hedin's function gives better agreement. The experimental line shape of the second and higher plasmon-loss lines cannot be described with self-convolutions of the line shape of the first plasmon-loss line. (iii) The same parameters as in case of the core levels describe the plasmon losses of the KLL and KLV Auger lines. (iv) The intrinsic plasmon excitation in case of photoemission from the valence band is markedly less: $\beta \simeq 0.10$. (v) In the Auger spectrum a plasmon gain peak of the $KL_{2,3}L_{2,3}$ (^1D) line is observed, again indicating a large contribution of the intrinsic plasmon excitation. (vi) The width of the plasmon-loss lines in EEL spectra decreases with increasing energy of the primary electrons. At 1200 eV the width of EEL plasmon-loss lines is considerably smaller than in the x-ray-photoelectron spectra. α is constant for the energy range 500–1500 eV and equal to $\alpha = 0.62 \pm 0.02$.

ACKNOWLEDGMENT

We gratefully acknowledge the technical assistance of A. E. M. Swolfs.

[1]D. Pines and D. Bohm, Phys. Rev. 85, 338 (1952).
[2]D. Bohm and D. Pines, Phys. Rev. 92, 609 (1953).
[3]D. Pines, *Elementary Excitations in Solids* (Benjamin, New York, 1964).
[4]H. Ehrenreich, H. R. Philipp, and B. Segall, Phys. Rev. 132, 1918 (1963).
[5]C. J. Powell and J. B. Swan, Phys. Rev. 115, 869 (1959).
[6]R. E. Burge and D. L. Misell, Philos. Mag. 18, 261 (1968).
[7]N. Swanson, J. Opt. Soc. Am. 54, 1130 (1964).
[8]Osamu Sueoka, J. Phys. Soc. Jpn. 20, 2203 (1965).
[9]Tetsuji Aiyama and Keiji Yada, J. Phys. Soc. Jpn. 36, 1554 (1974).
[10]W. J. Pardee, G. D. Mahan, D. E. Eastman, R. A. Pollak, L. Ley, F. R. McFeely, S. P. Kowalczyk, and D. A. Shirley, Phys. Rev. B 11, 3614 (1975).
[11]P. Steiner, H. Höchst, and S. Hüfner, Phys. Lett. A 61, 410 (1977).
[12]D. R. Penn, J. Vac. Sci. Technol. 14, 300 (1977).
[13]D. R. Penn, Phys. Rev. Lett. 38, 1429 (1977).
[14]D. R. Penn, Phys. Rev. Lett. 40, 568 (1977).
[15]H. G. Nöller, H. D. Polaschegg, and H. Schillalies, J. Electron Spectrosc. Relat. Phenom. 5, 705 (1974).
[16]P. M. Th. M. van Attekum and J. M. Trooster, J. Electron Spectrosc. Relat. Phenom. 11, 363 (1977).
[17]P. M. Th. M. van Attekum and J. M. Trooster (unpublished).
[18]J. C. Fuggle, E. Källne, L. M. Watson, and D. J. Fabian, Phys. Rev. B 16, 750 (1977).
[19]R. A. Pollak, L. Ley, F. R. McFeely, S. P. Kowalczyk, and D. A. Shirley, J. Electron Spectrosc. Relat. Phenom. 3, 381 (1974).
[20]S. A. Flodstrom, R. Z. Bachrach, R. S. Bauer, J. C. McMenamin, and S. B. M. Hagström, J. Vac. Sci. Technol. 14, 303 (1977).
[21]P. H. Citrin, G. K. Wertheim, and Y. Baer, Phys. Rev. B 16, 4256 (1977).
[22]L. H. Hedin, in *X-ray Spectroscopy*, edited by L. V. Azaroff (McGraw-Hill, New York, 1974), p. 226.
[23]F. James and M. Roos, Comput. Phys. Commun. 10, 343 (1975).
[24]R. S. Williams, S. P. Kowalczyk, P. S. Wehner, G. Apai, J. Stöhr, and D. A. Shirley, J. Electron Spectrosc. Relat. Phenom. 12, 477 (1977).
[25]G. D. Mahan, Phys. Status Solidi B 55, 703 (1973).

[26]Y. Baer and G. Busch, Phys. Rev. Lett., 30, 280 (1973).
[27]G. Dufour, J. -M. Mariot, P. -E. Nilsson-Jatko, and R. C. Karnatak, Phys. Scr. 13, 370 (1976).
[28]L. Ley, F. R. McFeely, S. P. Kowalczyk, J. G. Jenkin, and D. A. Shirley, Phys. Rev. B 11, 600 (1975).
[29]J. C. Fuggle, L. M. Watson, P. R. Norris, and D. J. Fabian, J. Phys. F 5, 590 (1975).
[30]G. A. Sawatzky, Phys. Rev. Lett. 39, 504 (1977).
[31]P. M. Th. M. van Attekum and J. M. Trooster (unpublished).
[32]G. Dufour, H. Guennou, and C. Bonnelle, Surf. Sci. 32, 731 (1972).
[33]L. H. Jenkins and M. F. Chung, Surf. Sci. 33, 159 (1972).
[34]M. Suleman and E. B. Pattinson, J. Phys. F 1, L21 (1971).
[35]H. Löfgren and L. Wallden, Solid State Commun. 12, 19 (1973).
[36]J. E. Rowe and S. B. Christman, Solid State Commun. 13, 315 (1973).
[37]C. M. K. Watts, J. Phys. F 2, 574 (1972).
[38]C. O. Almbladh, Nuovo Cimento B 23, 75 (1974).
[39]J. C. Fuggle, D. J. Fabian, and L. M. Watson, J. Electron Spectrosc. Relat. Phenom. 9, 99 (1976).
[40]H. Höchst, P. Steiner, and S. Hüfner, J. Phys. F 7, L309 (1977).
[41]P. C. Gibbons, S. E. Schnatterly, J. J. Ritsko, and J. R. Fields, Phys. Rev. B 13, 2451 (1976).
[42]D. Langreth, in *Collective Properties of Physical Systems*, edited by B. and S. Lundqvist (Academic, New York, 1974).
[43]J. W. Gadzuk, J. Electron Spectrosc. Relat. Phenom. 11, 355 (1977).